FEBS Letters 586 (2012) 3097–3103

FEBS Letters
journal homepage: www.FEBSLetters.org

Comparative analysis of two glyceraldehyde-3-phosphate dehydrogenases from a thermoacidophilic archaeon, *Sulfolobus tokodaii*

Fumiaki Ito, Hidehiro Chishiki, Shinya Fushinobu, Takayoshi Wakagi *

Department of Biotechnology, The University of Tokyo, 1-1-1 Yayoi, Bunkyo-ku, Tokyo 113-8657, Japan

ARTICLE INFO

Article history:
Received 27 April 2012
Revised 13 July 2012
Accepted 15 July 2012
Available online 27 July 2012

Edited by Miguel De la Rosa

Keywords:
Glyceraldehyde-3-phosphate dehydrogenase
Allosteric enzyme
Archaea

ABSTRACT

Sulfolobus tokodaii, a thermoacidophilic archaeon, possesses two structurally and functionally different enzymes that catalyze the oxidation of glyceraldehyde-3-phosphate (GAP): non-phosphorylating GAP dehydrogenase (St-GAPN) and phosphorylating GAP dehydrogenase (St-GAPDH). In contrast to previously characterized GAPN from _Sulfolobus solfataricus_, which exhibits V-type allosterism, St-GAPN showed K-type allosterism in which the positive cooperativity was abolished with concomitant activation by glucose 1-phosphate (G1P). St-GAPDH catalyzed the reversible oxidation of GAP to 1,3-bisphosphoglycerate (1,3-BPG) with high gluconeogenic activity, which was specific for NADPH, while both NAD^+ and $NADP^+$ were utilized in the glycolytic direction.

Structured summary of protein interactions:
GAPDH and GAPDH bind by molecular sieving (View interaction)
GAPN and GAPN bind by 2.2molecular sieving (View interaction).

1. Introduction

The archaeal glycolytic pathway is divergent. In the *Sulfolobales*, thermoacidophilic archaea, the semi-phosphorylative variant of the Entner–Doudoroff pathway (spED pathway), as well as the non-phosphorylative variant (npED pathway), for glycolysis has been reported [1–5]. In the spED pathway, glyceraldehyde-3-phosphate (GAP) is oxidized by two structurally and functionally different enzymes: non-phosphorylating GAP dehydrogenase (GAPN) and classical phosphorylating GAP dehydrogenase (GAPDH) [6,7]. GAPN exhibits no sequence homology with GAPDH. GAPN is present in most archaea, and certain groups of bacteria and eukaria [7–9], whereas GAPDH is ubiquitous in all three domains [10,11].

GAPN catalyzes the irreversible, non-phosphorylating oxidation of GAP to 3-phosphoglycerate (3-PG). Previously, the allosteric properties of GAPNs from archaea including *Thermoproteus tenax* (Ttx-GAPN), *Sulfolobus solfataricus* (Sso-GAPN), and *Thermococcus kodakarensis* (Tko-GAPN) were reported, which are homotetrameric and show significant activation by glucose 1-phosphate (G1P) [12–14]. The substrate, co-substrate and effector binding sites were identified in Ttx-GAPN, whose crystal structure is the only one known among archaeal GAPNs [15,16]. In this structure, a conformational change is not observed upon the binding of an effector and how effectors contribute to the allosteric activation remains unclear.

GAPDH catalyzes the reversible, phosphorylating oxidation of GAP to 1,3-bisphosphoglycerate (1,3-BPG). Hence, GAPDH is responsible for both glycolysis and gluconeogenesis. The archaeal GAPDHs belong to a different class of enzyme to their bacterial and eukaryotic counterparts, due to the low overall sequence identity (16–20%) [17–21]. In contrast to the bacterial and eukaryotic GAPDHs, which are usually specific for NAD^+, archaeal GAPDHs utilize both $NADP^+$ and NAD^+ in the glycolytic direction [17,21]. But there is little information on the gluconeogenic reactions of archaeal GAPDHs, especially on co-substrate usage. GAPDHs are homotetrameric.

In this study we purified GAPN from *Sulfolobus tokodaii* and characterized the recombinant enzyme. In contrast to the previously characterized GAPN from *Sulfolobus solfataricus* that shows V-type allosteric behavior, being the maximal velocity increased five fold by G1P without a change in affinity (K_m value) for substrate GAP, St-GAPN showed K-type allosteric behavior, being the strong positive cooperativity for GAP abolished with a significant increase in affinity for GAP. GAPN variants that showed altered dependence on NAD/NADP were also constructed. On the

Abbreviations: ED, Entner–Doudoroff; npED pathway, non-phosphorylative ED pathway; spED pathway, semi-phosphorylative ED pathway; GAP, glyceraldehyde-3-phosphate; G1P, glucose 1-phosphate; 1,3-BPG, 1,3-bisphosphoglycerate; GAPN, non-phosphorylating GAP dehydrogenase; GAPDH, phosphorylating GAP dehydrogenase; GNOR, GAP:$NADP^+$ oxidoreductase

* Corresponding author. Fax: +81 3 5841 5152.
E-mail address: atwakag@mail.ecc.u-tokyo.ac.jp (T. Wakagi).

0014-5793/$36.00
http://dx.doi.org/10.1016/j.febslet.2012.07.059

other hand, the recombinant St-GAPDH showed unique co-substrate usage; the enzyme can use both NAD^+ and $NADP^+$ in the forward direction but only NADPH in the reverse direction, exhibiting high activity.

2. Materials and methods

2.1. Chemicals

D,L-GAP, 3-PG, and phosphoglycerate kinase (PGK) from *Saccharomyces cerevisiae* were purchased from Sigma–Aldrich. NAD^+, $NADP^+$, NADH, NADPH and ATP were purchased from Oriental Yeast.

2.2. Strains and growth conditions

S. tokodaii was grown in a nutrient medium at pH 3 and 75 °C, as described previously [22]. *Escherichia coli* strains XL10 GOLD and C43 (DE3), for cloning and expression, respectively, were cultured in Luria–Bertani (LB) medium.

2.3. Purification of GAP:$NADP^+$ oxidoreductase (GNOR)

S. tokodaii cells (100 g wet weight) were harvested at the late exponential phase, suspended in 500 ml of buffer composed of 50 mM Tris–HCl (pH 8.0), 0.5 mM phenylmethylsulfonyl fluoride (PMSF), and a trace amount of DNaseI, and then disrupted by sonication. The cell lysate was centrifuged at 20,000*g* for 60 min at 15 °C, and the supernatant was dialysed against 20 mM Tris–HCl (pH 7.5) and applied to a Q-Sepharose column (240 ml, GE Healthcare) equilibrated with 30 mM Tris–HCl (pH 8.5). The active fraction was eluted using a linear gradient of NaCl, from 0 to 500 mM. Ammonium sulfate was added to a final concentration of 1.2 M to the fraction, and the sample was loaded onto a Butyl Toyopearl column (24 ml TOSOH) equilibrated with 20 mM Tris–HCl (pH 8.5) containing 1.2 M ammonium sulfate. The active fraction was eluted using a linear gradient of ammonium sulfate, from 1.2 to 0 M, dialysed against 20 mM sodium phosphate (pH 7.7), and then applied to a hydroxyapatite column (5 ml, Bio Rad) equilibrated with 20 mM sodium phosphate (pH 7.7). The active fraction was eluted using a linear gradient of sodium phosphate, from 20 to 240 mM. The active fraction was concentrated using a Centrifugal Filter Unit (Millipore), and applied to a Superdex 200 10/300 column (GE Healthcare) equilibrated with 20 mM Tris–HCl (pH 8.5) containing 150 mM NaCl. The active fraction was concentrated using a concentrator membrane and then applied to a MonoQ column (GE Healthcare) equilibrated with 30 mM Tris–HCl (pH 8.0). The active fraction was eluted using a linear gradient of NaCl, from 0 to 500 mM. The active fraction was concentrated using a concentrator membrane, and then ammonium sulfate was added to a final concentration of 1.6 M. The sample was loaded onto a Phenyl Toyopearl column (5 ml, TOSOH) equilibrated with 20 mM Tris–HCl (pH 8.0) containing 1.6 M ammonium sulfate and eluted using a linear gradient of ammonium sulfate, from 1.6 to 0 M. The active fraction was concentrated using a concentrator membrane and stored at 4 °C until use. The N-terminal amino acid sequence was determined with a Procise HT (Applied Biosystems).

2.4. Construction of expression plasmids and site-directed mutagenesis

The *st1356* and *st2477* genes were amplified by PCR, and then inserted between the NdeI and XhoI sites of the pET21a expression vector (Novagen) to construct expression plasmids. The primers used were: 5′-GGGAATTC*CATATG*CACCACCACCACCACCACGAAAAA GTTAAGGTAGCTGTA-3′ and 5′-CCG*CTCGAG*TCATAAT AGATACCCTT TCATAATTCC-3′ for *st1356*, and 5′-GGGAATTC*CATATG* CACCACCACCACCACCACGTTACTCTAAAA GAATTAAC TGG-3′ and 5′-CCG*CTCGAG*TTACAA GTACTCCCATACACCTT TACC-3′ for *st2477*, the NdeI and XhoI sites being in italics, and the introduced His-tag at the N-terminal being underlined. The S199I and A198S/S199I mutant versions of St-GAPN were constructed using a PrimeSTAR mutagenesis kit (Takara Bio) following the manufacturer's instructions, with the following primers: 5′-CCAGCTATCTCAACTCCCTTACCAGCA-3′ and 5′-AGTTGAGATAGCTGGCTTTAACATAAA-3′ for S199I, and 5′-AAGCCATCTATCTCAACTCCCTTACCA-3′ and 5′-TGAGATAGATGGCTTTAACATAAACGC-3′ for A198S/S199I.

2.5. Recombinant protein expression and purification

Recombinant *Escherichia coli* C43 (DE3) strains were cultured in LB medium containing 0.1 mg/mL ampicillin at 37 °C until OD600 = 0.6, when 1 mM isopropyl-β-thiogalactoside (IPTG) was added, followed by further cultivation at 30 °C for 21 h. Recombinant *E. coli* cells (1 g wet weight) were suspended in 20 mM Tris–HCl (pH 7.5) containing 0.2 mM PMSF, disrupted by sonication and then centrifuged (10,000*g* for 30 min at 4 °C). The resulting supernatant was incubated for 30 min at 80 °C and centrifuged (10,000*g* for 30 min at 4 °C). The supernatant containing the recombinant protein was applied to a HisTrap FF crude column (GE Healthcare) preequilibrated with 20 mM Tris–HCl (pH 7.5), and the column was washed with 40 mM imidazole and then eluted with 500 mM imidazole. The peak fraction was subjected to gel filtration on Superdex 200 10/300 GL (GE Healthcare) equilibrated with 20 mM Tris–HCl (pH 7.5) containing 150 mM NaCl. The fractions containing the homogeneous enzyme were pooled and used for characterization.

Protein concentrations were determined with a bicinchoninic acid (BCA) protein assay kit (Pierce) using bovine serum albumin as a standard.

2.6. Enzyme assays and determination of kinetic parameters

In the purification experiment, GNOR activity was assayed in a reaction mixture comprising 50 mM EPPS/NaOH (pH 8.0), 10 mM DL-GAP, 0.2 mM $NADP^+$ and 10 mM phosphate at 60 °C. The GAPN standard enzyme assay was performed in 50 mM EPPS/NaOH (pH 8.0) and 1 mM $NADP^+$ or 5 mM NAD^+ in a final volume of 400 μl at 60 °C. Reactions were started by the addition of DL-GAP (final concentration, 5 or 10 mM) in the presence of the purified enzyme after 100 s preincubation. The GAPDH activity in the forward direction was determined in 50 mM EPPS/NaOH (pH 8.0), 20 mMK-phosphate (pH8.0 adjusted by mixing KH_2PO_4 and K_2HPO_4), and 0.5 mM $NADP^+$ or 10 mM NAD^+ in a final volume of 400 μl at 60 °C. The GAPDH activity in the reverse direction was determined in 50 mM EPPS/NaOH (pH 8.0), 1 mM ATP, 1 mM $MgSO_4$, 1 mM EDTA, 10 mM 3-phosphoglycerate, 0.5 mM NADPH and phosphoglycerate kinase from *S. cerevisiae* (20 μg) in a final volume of 400 μl at 50 °C [23], because the coupling enzyme is not thermostable. Enzymatic activities were measured by monitoring the increase in NADPH or NADH at 340 nm. The kinetic parameters (V_{max} and K_m) were calculated by iterative curve-fitting using the program IGOR Pro (HULINKS).

3. Results

3.1. Purification of GNOR from S. tokodaii

A practically homogenous enzyme with GNOR activity was purified 108-fold from an *S. tokodaii* crude extract. A typical purification procedure is summarized in Supplementary Table S1. The sample gave a prominent 55 kDa band on a SDS–PAGE gel (Supplementary

Table 1
Molecular and catalytic properties of recombinant St-GAPN and St-GAPDH.

	St-GAPN(*st2477*)	St-GAPDH(*st1356*)
Length (aa)	506	343
Molecular mass (theoretical) (kDa)	56.4	37.5
Molecular mass (SDS–PAGE) (kDa)	56	38
Molecular mass (gel filtration) (kDa)	227	148
Oligomeric structure	α_4	α_4
Reversible/irreversible	Irreversible	Reversible
Cooperativity for GAP	+	–
Optimum pH at 60 °C	7.5	10.5[a]
Optimum temperature (°C)	85	95[a]

[a] Forward reaction.

Fig. S1). The molecular mass of the native enzyme determined by gel filtration (Superdex) was 223 kDa, suggesting a homotetrameric subunit composition. The N-terminal amino acid sequence was SVTLKELTGFK, which completely coincided with that of ST2477, annotated as non-phosphorylating NADP$^+$-dependent glyceraldehyde-3-phosphate dehydrogenase (St-GAPN). The theoretical molecular weight of St-GAPN is 56.4 kDa, which is in good agreement with the size determined on SDS–PAGE. Thus, the *S. tokodaii* crude extract contained mainly GAPN and negligible GAPDH. A kinetical study of the native St-GAPN showed highly positive cooperativity for GAP, unlike Sso-GAPN, so we constructed a recombinant St-GAPN and further characterized the enzyme (see below).

3.2. Characterization of native and recombinant St-GAPN (ST2477)

The purified recombinant St-GAPN showed a molecular mass of 56 kDa (theoretically, 56.4 kDa) on SDS–PAGE and that of 227 kDa on gel filtration (Table 1). The native and recombinant St-GAPNs showed similar tetrameric structures, co-substrate properties, overall saturation curve shape and allosteric properties (data not shown). The kinetic properties of the recombinant St-GAPN are shown below.

St-GAPN exhibited classical Michaelis–Menten kinetics for co-substrate NADP$^+$ (K_m of 0.023 ± 0.003 mM and V_{max} of 2.38 ± 0.04 U mg^{-1} protein), while NAD$^+$ was a poor co-substrate. The NAD$^+$-dependent reaction of St-GAPN showed no saturation up to 20 mM (Fig. 1). The apparent K_m value for NAD$^+$ is at least 1000-fold higher than that for NADP$^+$ (Table 2). Therefore, St-GAPN rather preferred NADP$^+$ to NAD$^+$ as a physiological co-substrate. This co-substrate preference of St-GAPN is different from that of Ttx-GAPN, which exhibits 2.6-fold higher velocity and 6.5-fold higher affinity with NAD$^+$ as the co-substrate compared to NADP$^+$ in the absence of effector [15].

The NADP$^+$-dependent DL-GAP saturation curves were sigmoidal with the excess of substrate causing inhibition (Fig. 2(a)). The DL-GAP curves resembled those of Tko-GAPN and were approximated by the four substrate binding site model proposed for the latter enzyme. Similarly to Tko-GAPN, the affinity for DL-GAP increased (K_s decreased from 625 to 0.42 mM) (Supplementary Table S2), the positive cooperativity was abolished (interaction coefficient increased from 0.066 to 1.13), and V_{max} increased by 1.4-fold with increasing G1P concentration from 0 to 100 μM. This is contrast to Sso-GAPN, which exhibits classical Michaelis–Menten kinetics for DL-GAP, and where effector G1P does not influence the affinity for DL-GAP but increases the turnover several fold.

In contrast, the NAD$^+$-dependent DL-GAP saturation curves were not sigmoidal (Fig. 2(b)). G1P (0.1 mM) activated the reaction but excess DL-GAP caused considerable inhibition. Maximum velocity was observed at around 0.5 mM DL-GAP in both the presence and absence of G1P.

In the co-substrate saturation curves, the maximal velocity increased by eight fold without a change in the affinity for NADP$^+$, while only low activation was observed for NAD$^+$ on the addition of G1P at 5 mM DL-GAP (Fig. 1 and Table 2). Of the other metabolites tested, a slight increase in St-GAPN activity was observed in the presence of fructose 6-phosphate and coenzyme A (1.1-fold). The following compounds exhibited no effect on St-GAPN: ATP, ADP, AMP, glucose 6-phosphate and galactose 1-phosphate.

3.3. Shifting the co-substrate preference in GAPN

In the present study, St-GAPN showed a preference for NADP$^+$ (k_{cat}/K_m of 96.6 s^{-1} mM^{-1}) over NAD$^+$ (k_{cat}/K_m of 0.378 s^{-1} mM^{-1}). In contrast to St-GAPN, Ttx-GAPN prefers NAD$^+$ in the absence of an effector but utilizes NADP$^+$ only in the presence of an effector [15]. In the crystal structure of Ttx-GAPN, the co-substrate binding pocket was clearly identified and the residues responsible for recognition of the 2′ phosphate group of NADP$^+$ or the 2′ hydroxyl group of NAD$^+$ were proposed [15]. The 2′ phosphate group of NADP$^+$ is bound by the main chain nitrogen atoms of Gly224 (Gly229), Ile194 (Ser199), the side-chain of Ser193 (Ala198), and Lys191 (Lys196) (the corresponding residues in St-GAPN are shown in parentheses).

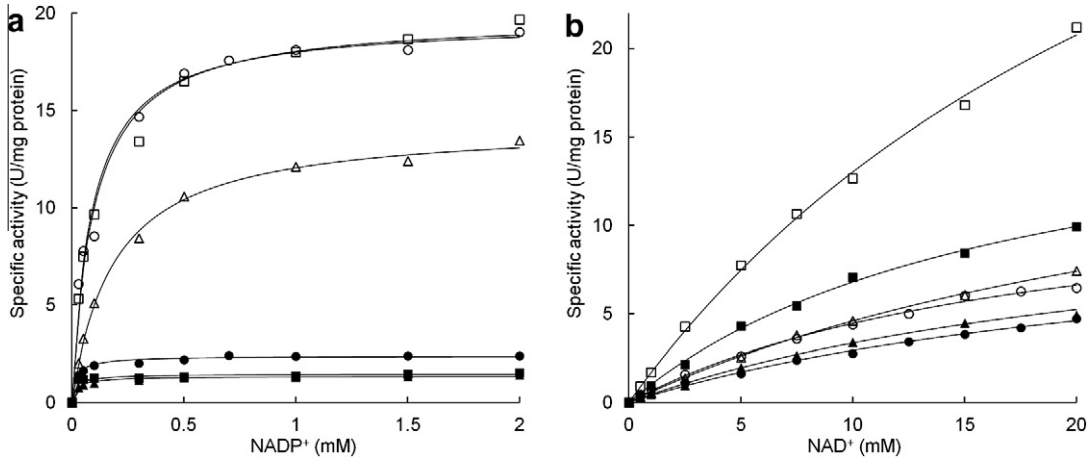

Fig. 1. Co-substrate dependence of St-GAPN. The reaction mixture contained NADP$^+$ (a) or NAD$^+$ (b), 5 mM DL-GAP, 0 mM (closed symbols) or 10 μM (open symbols) G1P and St-GAPN: wild type (circles), S199I (triangles), and A198S/S199I (squares). All data were fitted with Michaelis–Menten's equation. The calculated kinetic parameters are shown in Table 2.

Table 2
Kinetic parameters of wild type and mutant St-GAPNs.

Co-substrate	Enzyme	−G1P			+G1P (0.01 mM)		
		K_m (mM)	V_{max} (U/mg)	k_{cat}/K_m (s^{-1} mM^{-1})	K_m (mM)	V_{max} (U/mg)	k_{cat}/K_m (s^{-1} mM^{-1})
$NADP^+$	Wild type	0.0231 ± 0.0034	2.38 ± 0.04	96.6	0.0901 ± 0.0118	19.6 ± 0.5	203
	S199I	0.0263 ± 0.0043	1.34 ± 0.03	48.1	0.187 ± 0.012	14.3 ± 0.2	71.4
	A198S/S199I	0.0222 ± 0.0064	1.45 ± 0.06	61.5	0.0979 ± 0.0124	19.8 ± 0.5	188
NAD^+	Wild type	26.4 ± 6.3	10.7 ± 1.6	0.378	18.9 ± 2.4	12.9 ± 0.9	0.637
	S199I	25.8 ± 1.8	12.0 ± 0.5	0.434	19.4 ± 2.9	13.3 ± 1.2	0.639
	A198S/S199I	17.2 ± 1.6	18.5 ± 1.0	1.00	29.3 ± 3.4	51.2 ± 4.1	1.63

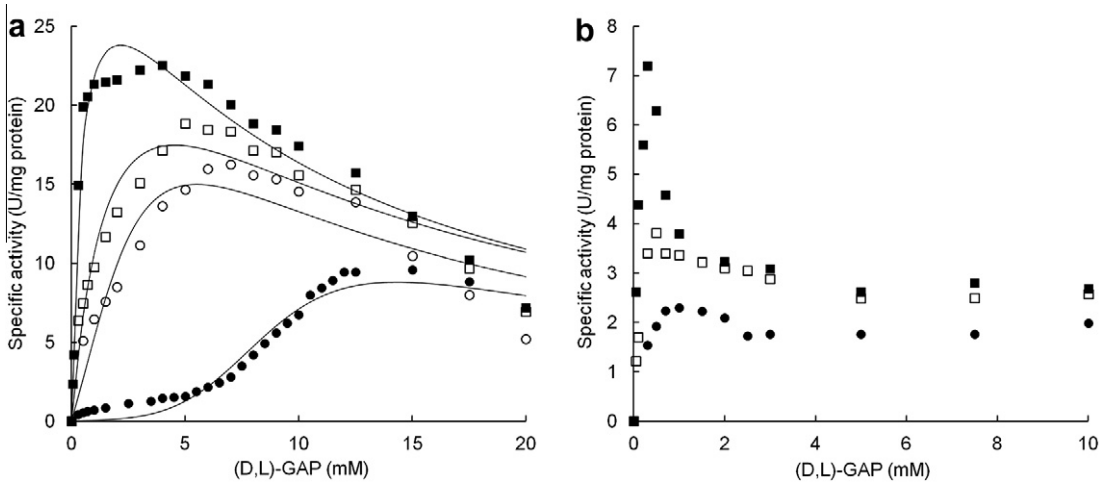

Fig. 2. DL-GAP dependence of St-GAPN with 1 mM $NADP^+$ (a) or 5 mM NAD^+ (b). The effector (G1P) concentrations were 0 (closed circles), 5 μM (open circles), 10 μM (open squares), and 100 μM (closed squares). The data in (a) were fitted with the equation based on the four substrate binding site model proposed for Tko-GAPN [14]. The calculated kinetic parameters are shown in Table S2.

In order to identify the residues that determine the co-substrate preference, we constructed the S199I and A198S/S199I mutants of St-GAPN mimicking Ttx-GAPN. The kinetic values for the two mutants (S199I and A198S/S199I) are summarized in Table 2. Mutations at these positions affected the co-substrate preference to some degree (Fig. 1). For S199I, the catalytic efficiency (k_{cat}/K_m) with $NADP^+$ decreased by 0.5-fold while that with NAD^+ remained unchanged. For A198S/S199I, the catalytic efficiency with $NADP^+$ decreased while that with NAD^+ increased by 2.5-fold (Table 2). The S199I and A198S/S199I substitutions reduced the NADP/NAD preference ratio by more than 50%. In particular, the latter substitution reduced the value by more than 75% in the absence of G1P (Table 3).

Thus, mutational analysis of St-GAPN suggested that Ala198 and Ser199 affect the co-substrate specificity to some degree, but these residues are clearly not the only ones determining the co-substrate specificity. Our results indicate that the S199I mutation is responsible for exclusion of $NADP^+$, suggesting that the side chain hydroxyl group of Ser199 may coordinate with the 2′ phosphate group of $NADP^+$ (Supplementary Fig. S2).

Table 3
Co-substrate preferences of wild type and mutant St-GAPNs and archaeal GAPNs.

Enzyme	NADP/NAD ratio[a]	
	−G1P	+G1P
Wild type St-GAPN	255	319
S199I	111	112
A198S/S199I	61	115
Ttx-GAPN[b]	0.06	4.9

[a] Ratio of k_{cat}/K_m for $NADP^+$ per k_{cat}/K_m for NAD^+.
[b] From Lorentzen et al. 2004.

3.4. Characterization of recombinant St-GAPDH (ST1356)

Unlike GAPN, GAPDH requires inorganic phosphate (Pi) for its glycolytic reaction. The St-GAPDH reaction was Pi-dependent and showed no saturation even with 55 mM Pi (where the activity was 16.1 U mg^{-1} protein in the presence of 10 mM DL-GAP and 1 mM $NADP^+$) (Supplementary Fig. S3). We measured the St-GAPDH activity in both the glycolytic and gluconeogenic directions. The St-GAPDH activity in the glycolytic direction was measured in the presence of 0.5 mM $NADP^+$ and 20 mM Pi at 60 °C (K_m of 0.21 ± 0.04 mM and V_{max} of 11.7 ± 0.7 U mg^{-1} protein) (Fig. 3(a)). In this direction, St-GAPDH seems to reach an equilibrium state within 1 min. The St-GAPDH activity in the gluconeogenic direction was measured by means of a coupling assay with PGK from *S. cerevisiae* in the presence of 1 mM ATP and 0.5 mM NADPH at 50 °C. The maximal velocity of the reaction was 19.9 ± 0.5 U mg^{-1} protein, which is more than two fold higher than in the glycolytic direction (Fig. 3(b)). St-GAPDH activity in the gluconeogenic direction was 14-fold higher than that in the glycolytic direction when both activities were measured at 50 °C in the presence of 10 mM substrate and 0.5 mM co-substrate (data not shown). Thus, St-GAPDH showed a higher preference for gluconeogenesis, although it can catalyze the reaction reversibly. We next studied the co-substrate preference of St-GAPDH. In the $NADP^+$-dependent reaction, St-GAPDH showed the highest activity of 3.9 U/mg with 0.5 mM $NADP^+$ in the presence of 10 mM DL-GAP and 10 mM Pi. In the NAD^+-dependent reaction, St-GAPDH showed the highest activity of 4.5 U/mg with 15 mM NAD^+ in the presence of 10 mM DL-GAP

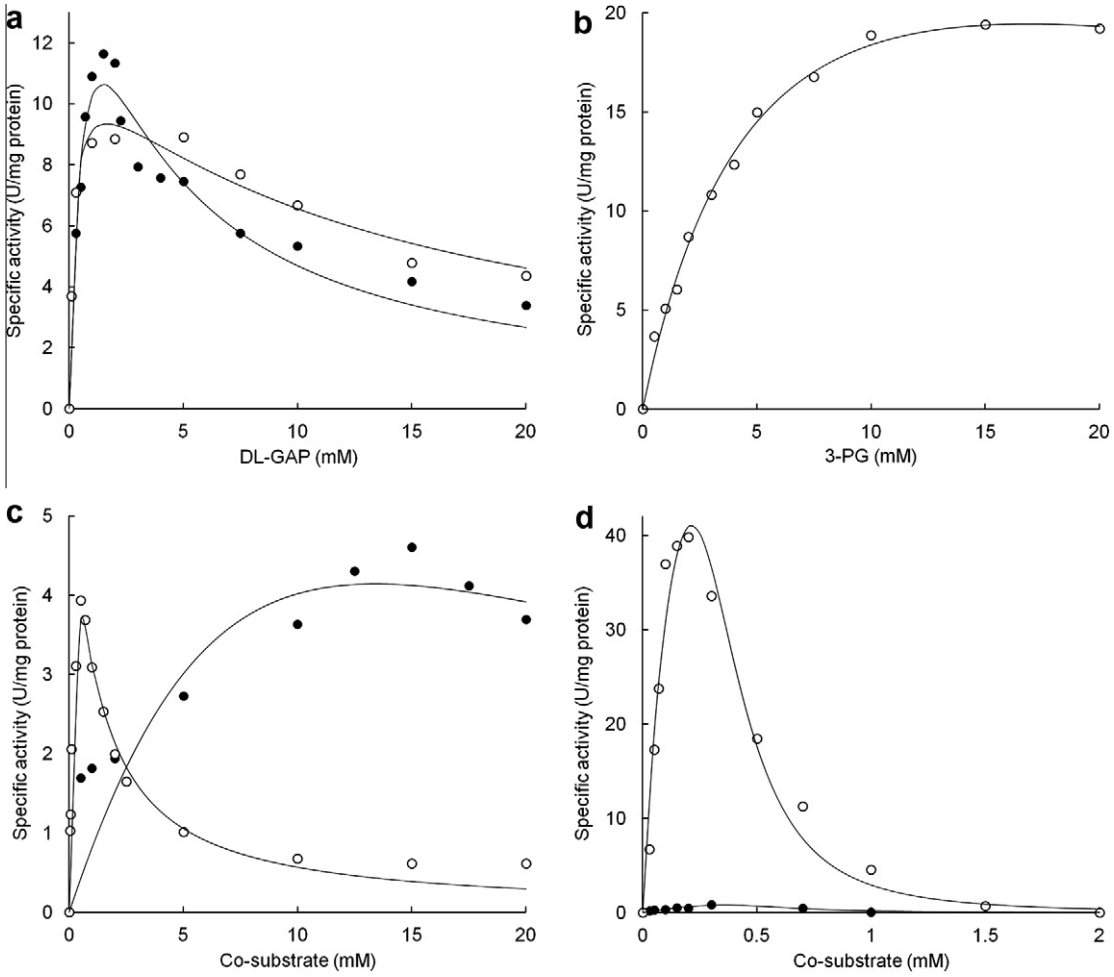

Fig. 3. Substrate dependence of St-GAPDH in the forward (a) and reverse (b) directions with 0.5 mM $NADP^+$ (or NADPH) (open circles) or 5 mM NAD^+ (closed circles), and co-substrate dependence of St-GAPDH in the forward (c) and reverse (d) directions with $NADP^+$ (or NADPH) (open symbols) and NAD^+ (or NADH) (closed symbols). The details of data fitting and the experimental conditions are summarized in Table 4.

and 10 mM Pi (Fig. 3(c)). The highest activity is almost equal for $NADP^+$ and NAD^+, whereas the affinity for $NADP^+$ is higher than that for NAD^+. However, in the gluconeogenic direction, St-GAPDH showed a strong preference for NADPH, and only negligible activity was detected with NADH in the concentration range of 0–1 mM (Fig. 3(d)). In both cases, strong inhibition with excess co-substrate was observed and no activity was observed with over 2 mM NADH or NADPH. Thus, St-GAPDH utilized almost only NADPH as a co-substrate in the gluconeogenic direction. The kinetic parameters are summarized in Table 4.

The activity of St-GAPDH proved to be insensitive to various metabolites and intermediates. No influence on activity was observed on assaying of the enzyme with 5 mM substrate and 0.5 mM co-substrate with 1 mM ATP, ADP, AMP, glucose 6-phosphate, fructose 6-phosphate, galactose 1-phosphate, glucose 1-phosphate or coenzyme A in either the glycolytic or gluconeogenic reaction.

Table 4
Kinetic parameters of phosphorylating glyceraldehyde 3-phosphate dehydrogenase (St-GAPDH) for the oxidative and reductive reactions. For DL-GAP, NAD^+, $NADP^+$ and 3-PG, the kinetic parameters were calculated using the equation based on the single inhibitory site model: $v = V_{max}/(K_m/[S] + 1 + [S]/K_i)$. For NADH and NADPH, the kinetic parameters were calculated using the equation based on the three inhibitory sites model: $v = V_{max}/(K_m/[S] + 1 + [S]^3/K_{i1}K_{i2}K_{i3})$. For phosphate, the kinetic parameters were calculated using Michaelis–Menten's equation.

Direction	Variable substrate	Fixed substrate	K_m (mM)	V_{max} (U/mg)	K_i (mM)
Oxidation[a]	DL-GAP	10 mM NAD^+, 20 mM phosphate	0.77 ± 0.28	21.8 ± 4.4	2.8 ± 0.9
	DL-GAP	0.5 mM $NADP^+$, 20 mM phosphate	0.21 ± 0.04	11.7 ± 0.7	13.1 ± 2.2
	Phosphate	10 mM DL-GAP, 1 mM $NADP^+$	107 ± 22	48.4 ± 7.4	-
	NAD^+	10 mM DL-GAP, 10 mM phosphate	16.8 ± 8.9	14.5 ± 5.5	10.7 ± 5.3
	$NADP^+$	10 mM DL-GAP, 10 mM phosphate	0.28 ± 0.08	8.2 ± 1.5	0.75 ± 0.21
Reduction[b]	3-PG	0.5 mM NADPH	5.8 ± 1.1	32.8 ± 4.1	49.1 ± 21.7
	NADH	10 mM 3-PG	0.61 ± 0.07	2.58 ± 0.18	0.081 ± 0.022[c]
	NADPH	10 mM 3-PG	0.18 ± 0.07	86.9 ± 22.1	0.035 ± 0.015[c]

[a] Measured at 60 °C.
[b] Measured at 50 °C.
[c] The value correspond to $K_{i1}K_{i2}K_{i3}$.

4. Discussion

In the present study, GAPN, but not GAPDH, was purified from a *S. tokodaii* crude extract, judging from the results of the GNOR activity assay applicable to both GAPDH and GAPN. This finding suggests that GAPN mainly catalyzes the glycolytic reaction in this step. In addition, a kinetic study of the recombinant St-GAPDH revealed that the enzyme exhibits higher activity in the gluconeogenic direction than in the glycolytic direction. Recently, the ⊿GADPH and ⊿GAPN strains of *T. kodakarensis* were constructed and their growth phenotypes were studied [14]. The ⊿GAPN strain showed no growth under glycolytic conditions whereas it grew well under gluconeogenic ones. In contrast, the ⊿GAPDH strain showed no growth under the gluconeogenetic conditions whereas it grew well under the glycolytic ones. Our results also suggest that GAPN absolutely fulfills the catabolic purpose whereas GAPDH exhibits anabolic features. Another marked feature of St-GAPDH is its unique co-substrate specificity; the enzyme utilized almost only NADPH as a co-substrate in the gluconeogenic direction, although it can utilize both NAD^+ and $NADP^+$ in the glycolytic direction. This unique co-substrate usage has not been reported for other archaeal GAPDHs. In the structure of GAPDH from *Methanothermus fervidus*, Lys33, Thr34 and Arg35 contribute to the recognition of the 2′ phosphate group of $NADP^+$ [24]. In St-GAPDH, the last arginine is replaced by serine. But how this binding mode contributes to the above unique co-substrate specificity remains unknown.

The most striking finding in this study is that St-GAPN showed different allosteric behavior from its highly close ortholog from *S. solfataricus* (Sso-GAPN) [13]. For St-GAPN, the increase in the affinity for substrate GAP on the binding of G1P to St-GAPN is more remarkable than the increase in the maximal velocity hence the allosteric effect of St-GAPN is of the K-type. In contrast, the allosteric behavior of Sso-GAPN is of the V-type since the maximal velocity increases on the addition of the same concentration of G1P by 5- to 6-fold without a change in the affinity (K_m value) for substrate GAP. This difference in the allosteric properties between St-GAPN and Sso-GAPN is quite notable in terms of both physiological and structural meaning since the two enzymes exhibit high homology (82% similarity and 66% identity) (See Fig. 4 and Supplementary Fig. S4). Intersubunit interaction may be involved in this difference regarding the positive cooperativity for substrate GAP and allosteric activation. Mutational analysis of the residues responsible for the cooperativity of St-GAPN is currently under way (Ito et al., unpublished work).

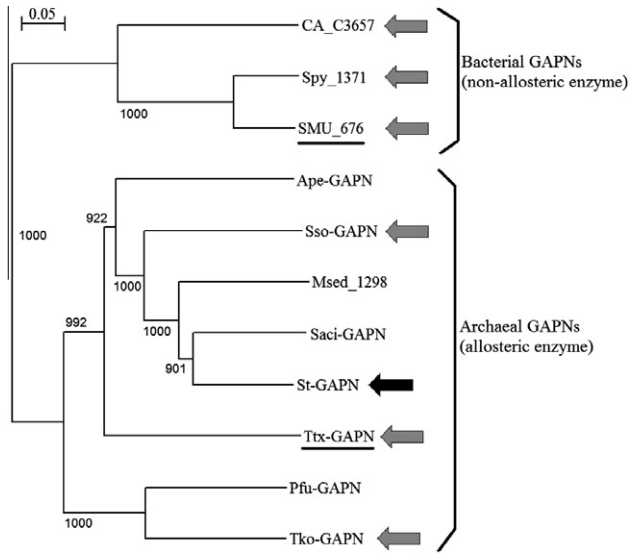

Fig. 4. Phylogenetic tree of archaeal and bacterial GAPNs. The tree was generated with Clustal W using the Neighbor Joining method and viewed with njplot. Bootstrap values obtained for 1000 pseudo-replicates of the data set are indicated only when the value was higher than 900. St-GAPN (ST2477) is indicated by a black arrow and the characterized proteins by grey arrows. Proteins for which the crystal structure has been solved are underlined. Bacterial GAPNs are reported to be non-allosteric enzymes. Species abbreviations: Sso: *Sulfolobus solfataricus*; St: *Sulfolobus tokodaii*; Saci: *Sulfolobus acidcaridarius;* CA: *Clostridium acetobutylicum*; Spy: *Streptococcus pyogenes*; SMU: *Streptococcus mutans*; Pfu: *Pyrococcus furiosus*; Tko: *Thermococcus kodakarensis*; Ttx: *Thermoproteus tenax*; Ape: *Aeropyrum pernix*; Msed: *Metallosphaera sedula*.

Acknowledgements

This work was supported by a Grant-in-aid for Scientific Research from the Japan Society for the Promotion of Science (to T.W., No. 120600000293).

Appendix A. Supplementary data

Supplementary data associated with this article can be found, in the online version, at http://dx.doi.org/10.1016/j.febslet.2012.07.059.

References

[1] Siebers, B. and Schonheit, P. (2005) Unusual pathways and enzymes of central carbohydrate metabolism in Archaea. Curr. Opin. Microbiol. 8, 695–705.
[2] Siebers, B., Tjaden, B., Michalke, K., Dorr, C., Ahmed, H., Zaparty, M., Gordon, P., Sensen, C.W., Zibat, A., Klenk, H.P., Schuster, S.C. and Hensel, R. (2004) Reconstruction of the central carbohydrate metabolism of *Thermoproteus tenax* by use of genomic and biochemical data. Arch. Microbiol. 186, 2179–2194.
[3] Verhees, C.H., Kengen, S.W., Tuininga, J.E., Schut, G.J., Adams, M.W., De Vos, W.M. and van der Oost, J. (2003) The unique features of glycolytic pathways in Archaea. Biochem. J. 375, 231–246.
[4] Albers, S.V., Birkeland, N.K., Driessen, A.J., Gertig, S., Haferkamp, P., Klenk, H.P., Kouril, T., Manica, A., Pham, T.K., Ruoff, P., Schleper, C., Schomburg, D., Sharkey, K.J., Siebers, B., Sierocinski, P., Steuer, R., van der Oost, J., Westerhoff, H.V., Wieloch, P., Wright, P.C. and Zaparty, M. (2009) SulfoSYS (*Sulfolobus* Systems Biology): towards a silicon cell model for the central carbohydrate metabolism of the archaeon *Sulfolobus solfataricus* under temperature variation. Biochem. Soc. Trans. 37, 58–64.
[5] Berg, I.A., Kockelkorn, D., Ramos-Vera, W.H., Say, R.F., Zarzycki, J., Hugler, M., Alber, B.E. and Fuchs, G. (2010) Autotrophic carbon fixation in archaea. Nat. Rev. Microbiol. 8, 447–460.
[6] Brunner, N.A., Siebers, B. and Hensel, R. (2001) Role of two different glyceraldehyde-3-phosphate dehydrogenases in controlling the reversible Embden-Meyerhof-Parnas pathway in *Thermoproteus tenax*: regulation on protein and transcript level. Extremophiles 5, 101–109.
[7] Crow, V.L. and Wittenberger, C.L. (1979) Separation and properties of NAD^+- and $NADP^+$-dependent glyceraldehyde-3-phosphate dehydrogenases from *Streptococcus mutans*. J. Biol. Chem. 254, 1134–1142.
[8] Iddar, A., Valverde, F., Assobhei, O., Serrano, A. and Soukri, A. (2005) Widespread occurrence of non-phosphorylating glyceraldehyde-3-phosphate dehydrogenase among gram-positive bacteria. Int. Microbiol. 8, 251–258.
[9] Piattoni, C.V., Rius, S.P., Gomez-Casati, D.F., Guerrero, S.A. and Iglesias, A.A. (2010) Heterologous expression of non-phosphorylating glyceraldehyde-3-phosphate dehydrogenase from *Triticum aestivum* and *Arabidopsis thaliana*. Biochimie 92, 909–913.
[10] Cori, C.F., Velick, S.F. and Cori, G.T. (1950) The combination of diphosphopyridine nucleotide with glyceraldehyde phosphate dehydrogenase. Biochim. Biophys. Acta 4, 160–169.
[11] Littlechild, J.A. and Isupov, M. (2001) Glyceraldehyde-3-phosphate dehydrogenase from *Sulfolobus solfataricus*. Methods Enzymol. 331, 105–117.
[12] Brunner, N.A., Brinkmann, H., Siebers, B. and Hensel, R. (1998) NAD^+-dependent glyceraldehyde-3-phosphate dehydrogenase from *Thermoproteus tenax*. The first identified archaeal member of the aldehyde dehydrogenase superfamily is a glycolytic enzyme with unusual regulatory properties. J. Biol. Chem. 273, 6149–6156.
[13] Ettema, T.J., Ahmed, H., Geerling, A.C., van der Oost, J. and Siebers, B. (2008) The non-phosphorylating glyceraldehyde-3-phosphate dehydrogenase (GAPN) of *Sulfolobus solfataricus*: a key-enzyme of the semi-phosphorylative branch of the Entner-Doudoroff pathway. Extremophiles 12, 75–88.
[14] Matsubara, K., Yokooji, Y., Atomi, H. and Imanaka, T. (2011) Biochemical and genetic characterization of the three metabolic routes in *Thermococcus kodakarensis* linking glyceraldehyde 3-phosphate and 3-phosphoglycerate. Mol. Microbiol. 81, 1300–1312.
[15] Lorentzen, E., Hensel, R., Knura, T., Ahmed, H. and Pohl, E. (2004) Structural Basis of allosteric regulation and substrate specificity of the non-

phosphorylating glyceraldehyde 3-Phosphate dehydrogenase from *Thermoproteus tenax*. J. Mol. Biol. 341, 815–828.
[16] Pohl, E., Brunner, N., Wilmanns, M. and Hensel, R. (2002) The crystal structure of the allosteric non-phosphorylating glyceraldehyde-3-phosphate dehydrogenase from the hyperthermophilic archaeum *Thermoproteus tenax*. J. Biol. Chem. 277, 19938–19945.
[17] Fabry, S. and Hensel, R. (1987) Purification and characterization of D-glyceraldehyde-3-phosphate dehydrogenase from the thermophilic archaebacterium *Methanothermus fervidus*. Eur. J. Biochem. 165, 147–155.
[18] Hensel, R., Laumann, S., Lang, J., Heumann, H. and Lottspeich, F. (1987) Characterization of two D-glyceraldehyde-3-phosphate dehydrogenases from the extremely thermophilic archaebacterium *Thermoproteus tenax*. Eur. J. Biochem. 170, 325–333.
[19] Jia, B., Linh le, T., Lee, S., Pham, B.P., Liu, J., Pan, H., Zhang, S. and Cheong, G.W. (2011) Biochemical characterization of glyceraldehyde-3-phosphate dehydrogenase from *Thermococcus kodakarensis* KOD1. Extremophiles 15, 337–346.
[20] Pruss, B., Meyer, H.E. and Holldorf, A.W. (1993) Characterization of the glyceraldehyde 3-phosphate dehydrogenase from the extremely halophilic archaebacterium *Haloarcula vallismortis*. Arch. Microbiol. 160, 5–11.
[21] Zwickl, P., Fabry, S., Bogedain, C., Haas, A. and Hensel, R. (1990) Glyceraldehyde-3-phosphate dehydrogenase from the hyperthermophilic archaebacterium *Pyrococcus woesei*: characterization of the enzyme, cloning and sequencing of the gene, and expression in *Escherichia coli*. Arch. Microbiol. 172, 4329–4338.
[22] Nishimasu, H., Fushinobu, S., Shoun, H. and Wakagi, T. (2006) Identification and characterization of an ATP-dependent hexokinase with broad substrate specificity from the hyperthermophilic archaeon *Sulfolobus tokodaii*. Arch. Microbiol. 188, 2014–2019.
[23] Furfine, C.S. and Velick, S.F. (1965) The Acyl-enzyme Intermediate and the Kinetic Mechanism of the Glyceraldehyde 3-Phosphate Dehydrogenase Reaction. J. Biol. Chem. 240, 844–855.
[24] Charron, C., Talfournier, F., Isupov, M.N., Littlechild, J.A., Branlant, G., Vitoux, B. and Aubry, A. (2000) The crystal structure of d-glyceraldehyde-3-phosphate dehydrogenase from the hyperthermophilic archaeon *Methanothermus fervidus* in the presence of $NADP^+$ at 2.1 Å resolution. J. Mol. Biol. 297, 481–500.